https://doi.org/10.5194/amt-2020-194
Preprint. Discussion started: 2 July 2020

Atmospheric Measurement Techniques Discussions

Verification of the AIRS and MLS ozone algorithms based on retrieved daytime and nighttime ozone

Wannan Wang[1,2,3], Tianhai Cheng[1], Ronald van der A[3], Jos de Laat[3], and Jason E Williams[3]

[1]Aerospace Information Research Institute, Chinese Academy of Sciences, Beijing, 100094 China
[2]University of Chinese Academy of Sciences, Beijing, 100049, China
[3]Royal Netherlands Meteorological Institute (KNMI), De Bilt, 3730 AE, the Netherlands

Correspondence to: Tianhai Cheng (chength@radi.ac.cn)

Abstract. Ozone (O_3) plays a significant role in weather and climate on regional to global spatial scales. Most studies on the variability in the total column of O_3 (TCO) are typically analysed using daytime data. Based on knowledge of the chemistry and transport of O_3, significant deviations between daytime and nighttime O_3 are only expected either in the planetary boundary layer (PBL) or high in the stratosphere or mesosphere, having little effect on the TCO. Hence, we expect the daytime and nighttime TCO to be very similar. Comparing daytime and nighttime TCOs thus provides an approach to verify the retrieval algorithms of infrared instruments like the Atmospheric InfraRed Sounder (AIRS) and the Microwave Limb Sounder (MLS). Applying this verification on the AIRS and the MLS data we identified inconsistencies in observations of O_3 from both satellite instruments. For AIRS, daytime-nighttime differences were found over oceans resembling cloud cover patterns, and over land, mostly over dry land areas, likely related to infrared surface emissivity. These differences point to issues with the representation of both processes in the AIRS retrieval algorithm. For MLS, a major issue was identified with the "ascending-descending" orbit flag, used to discriminate nighttime and daytime MLS measurements. Disregarding this issue, MLS day-night differences were significantly smaller than AIRS day-night differences, providing additional support for retrieval method origin of AIRS day-night TCO differences. MLS day-night differences are dominated by the upper stratospheric and mesospheric diurnal O_3 cycle. These results provide useful information for improving infrared O_3 products and at the same time will allow study the day-night differences of stratospheric and mesospheric O_3.

1 Introduction

Atmospheric ozone (O_3) is a key factor in the structure and dynamics of the Earth's atmosphere (London 1980). The 1987 Montreal Protocol on Substances that Deplete the O_3 Layer formally recognized the significant threat of the chlorofluorocarbons and the other O_3-depleting substances (ODCs) to the O_3 layer and marks the start of joint international efforts to reduce and ultimately phase-out the global production and consumption of ODCs (Velders et al., 2007). Indeed, concerns about changes in O_3 due to catalytic chemistry involving man-made chlorofluorocarbons has become as an important topic for the scientific community, the general public and governments (Fioletov et al., 2002).

https://doi.org/10.5194/amt-2020-194
Preprint. Discussion started: 2 July 2020

Atmospheric Measurement Techniques Discussions

In response to this concern and associated environmental policies, during the last two decades a large number of studies have focused on estimating long-term variations and trends in stratospheric column of O_3 (SCO). A summary of the state of the science is frequently reported in the quadrennial O_3 Assessment Reports issued by the United Nations Environmental Program (UNEP) and the World Meteorological Organization (WMO). These reports are written in response to the global treaties aiming at minimizing emissions of ODSs. The signatories of these treaties ask for regular updates on the state of the science and knowledge. The most recent O_3 Assessment reports extensively discuss long-term variations and trends in stratospheric O_3 in relation to expected recovery (WMO, 2011, 2014, 2018). According to WMO (2018), Antarctic stratospheric O_3 has started to recover, while outside of the polar regions, upper stratospheric O_3 has also increased. On the other hand, no significant trend has been detected in global (60°S-60°N) total column O_3 over the 1997-2016 period with average values for the years since the last Assessment remaining roughly 2% below the 1964-1980 average. Moreover, recently a debate has emerged over the question as to whether lower stratospheric O_3 between 60°S-60°N has continued to decline despite decreasing O_3 depleting substances (Ball et al., 2018; Ball et al., 2019). In addition to the quadrennial O_3 Assessments, the Bulletin of the American Meteorological Society annually publishes its "State of the Climate", which since 2015 includes a description of the relevant stratospheric events of the past year, the state of the Antarctic O_3 hole, as well as an annual update of global and zonal trends in stratospheric O_3. These regularly recurring reports and publications illustrate the continued attention and monitoring of the O_3 layer and its recovery, in which the long records of satellite observations play a crucial role. Establishing and maintaining the quality of the satellite observations of stratospheric O_3 is therefore highly relevant.

A variety of techniques exist to measure the O_3 column and stratospheric O_3. The UV absorption spectroscopy with the sun or stars as sources of UV light is the most used to derive O_3 (Weeks et al., 1978; Fussen et al., 2000). In addition to the UV occultation, the absorption of infrared radiation has also been used to detect O_3 profiles throughout the column (Gunson et al., 1990; Brühl et al., 1996). Another technique is the detection of the molecular oxygen dayglow emissions (Mlynczak and Drayson, 1990; Marsh et al., 2002). Some ground-based instruments use O_3 emissions in the microwave region to infer the O_3 density in the mesosphere (Zommerfelds et al., 1989; Connor et al., 1994). Infrared emission measurements overcome the limitations in the local time coverage of solar occultation and dayglow technique and their altitude resolution is significantly higher compared with microwave measurements (Kaufmann et al., 2003). The strongest O_3 infrared absorption centers near 9.6 um.

Based on knowledge of chemistry and transport of O_3, significant deviations between daytime and nighttime O_3 are only expected either in the planetary boundary layer (PBL) and high in the stratosphere or mesosphere, having little effect on the total column of O_3 (TCO). Hence, we expect that the daytime and nighttime TCO to be very similar. Day-night inter-comparisons present a unique opportunity to assess the internal consistency of infrared O_3 instruments (Brühl et al., 1996; Parrish et al., 2014). Temperature effects within satellite instruments, calibration procedures between day and night or inversion algorithms could potentially result in systematic differences between TCO measurements from different satellites. The Stratosphere Aerosol and Gas Experiment (SAGE) applied day-night differences to validate O_3 profiles and found daytime data have a low bias due to the retrieval method since the magnitude of the difference was much less in a photochemical model

https://doi.org/10.5194/amt-2020-194
Preprint. Discussion started: 2 July 2020

(Cunnold et al., 1989). There are infrared satellite instruments, like Atmospheric InfraRed Sounder (AIRS), and The Microwave Limb Sounder (MLS), that provide global daytime and nighttime TCO/SCO and O_3 profile. Although their daytime O_3 retrievals have been validated (Livesey et al., 2008; Sitnov and Mokhov, 2016), day-night differences in TCO and SCO are still largely unexplored.

The O_3 diurnal cycle depends on latitude, weather and time. The variations of the diurnal cycle are less than 5% in the tropics and subtropics and increasing to more than 15% near the polar day terminator in the upper stratosphere (Frith et al., 2020). There exist diurnal variations in atmospheric O_3 at certain altitudes. There are two distinct O_3 maxima in the typical vertical profile of the O_3 volume mixing ratio, one in the stratosphere and one in the mesosphere. The secondary maximum in the mesosphere is present during both day and night (Evans and Llewellyn, 1972; Hays and Roble, 1973). Chapman (1930) revealed the photochemical scheme in the mesosphere. The reactions of Chapman cycle are important for us to understand diurnal O_3 variation.

$$O_2 + hv \rightarrow 2O(\lambda < 240nm) , \quad (1)$$

$$O + O_2 + M \rightarrow O_3 + M, \text{ (in which M stands for an air molecule)} \quad (2)$$

$$O_3 + O \rightarrow 2O_2 , \quad (3)$$

$$O_3 + hv \rightarrow O_2 + O(\lambda < 1140nm) , \quad (4)$$

In the daytime mesosphere, catalytic O_3 depletion by odd hydrogen has to be considered in addition to the Chapman cycle. The anticorrelation of O_3 and temperature is mainly due to the temperature dependence of the chemical rate coefficients (Craig and Ohring, 1958; Barnett et al., 1975). Huang et al. (2008) and Huang et al. (1997) found midnight O_3 increases in the mesosphere, based on SABER and MLS data, respectively. Zommerfelds et al. (1989) surmised that eddy transport may explain this increase, while Connor et al. (1994) stated that atmospheric tides are expected to cause systematic day-night variations.

During daytime, photolysis is the major loss process. The main nighttime O_3 source in the mesosphere is atomic oxygen, while its sinks are atomic hydrogen and atomic oxygen (Smith and Marsh, 2005). In addition to chemical reactions with active hydrogen and molecular, the turbulent mass transport also plays an important role in the explanation of the secondary O_3 maximum (Sakazaki et al., 2013; Schanz et al., 2014).

Tropospheric O_3 is mainly produced during chemical reactions when mixtures of organic precursors (CH_4 and non-methane volatile organic carbon, NMVOC), CO, and nitrogen oxides (or NOx), are exposed to the UV radiation in the troposphere (Simpson et al., 2014). At night, in the absence of the sunlight, there is no O_3 production, but surface O_3 deposition and dark reactions transform the NOx-VOC mixture and remove O_3. The dark chemistry affects O_3 and its key ingredients mainly depend on the reactions of two nocturnal nitrogen oxides, NO_3 (the nitrate radical) and N_2O_5 (dinitrogen pentoxide). NO_3 oxidizes VOC at night, while reaction of N_2O_5 with aerosol particles containing water removes NOx. Both processes remove O_3 as well at night (Brown et al., 2006).

https://doi.org/10.5194/amt-2020-194
Preprint. Discussion started: 2 July 2020

Atmospheric Measurement Techniques Discussions

The diurnal cycle of O_3 in the middle stratosphere had generally been considered small enough to be inconsequential, with known larger variations in the upper stratosphere and mesosphere (Prather, 1981; Pallister and Tuck, 1983). Later studies have highlighted observed and modelled peak-to-peak variations of the order of 5% or more in the middle stratosphere between 30 and 1 hPa (Sakazaki et al., 2013; Parrish et al., 2014; Schanz et al., 2014).

In terms of dynamics, vertical transport due to atmospheric tides is expected to contribute to diurnal O_3 variations at altitudes where background O_3 levels have a sharp vertical gradient (Sakazaki et al., 2013). The Brewer/Dobson circulation transports air upwards in the tropics, polewards and downwards at high latitudes, with stronger transport towards the winter pole (Chipperfield et al., 2017).

The main objective of this paper is to analyse day-night differences in the AIRS TCO and the MLS SCO, as well as in MLS upper atmospheric O_3 profiles. Section 2 discusses the data used. Section 3 presents results for AIRS, MLS, the comparison of AIRS with MLS, and an application of AIRS TCO data over the Pacific low O_3 regions to highlight how day-night differences affect use and interpretation of TCO data. Finally, section 4 ends the paper with a brief summary and conclusions.

2 Data

2.1 AIRS TCO retrievals

The AIRS satellite instrument was the first in a new generation of high spectral resolution infrared sounder instruments flown aboard the National Aeronautics and Space Administration (NASA) Earth Observing System (EOS) Aqua satellite (Divakarla et al., 2008). The AIRS radiance data at 9.6 μm band are used to retrieve column O_3 and O_3 profiles during both day and night (including the polar night) (Pittman et al., 2009; Fu et al., 2018). The AIRS V6 level 3 standard TCO products (2003-2018) comprising daily averaged measurements on the ascending and descending branches of an orbit with the quality indicators 'best' and 'good' and binned into 1°×1° (latitude × longitude) grid cells are used here. Outside of the polar zones (60°N-90°N and 90°S-60°S), ascending and descending correspond respectively to daytime (13:30 in local solar time) and nighttime (01:30 in local solar time). Hereafter we refer to "day" and "night" rather than ascending and descending over 60°S-60°N. In the polar zones, it is inappropriate to use ascending/descending mode to define daytime/nighttime, therefore, we just compare differences between ascending and descending mode. AIRS TCO measurements agree well with the global Brewer/Dobson Network station measurements with a bias of less than 4% and a root mean squared error (RMSE) difference of approximately 8% (Divakarla et al., 2008). Analysis of AIRS TCO monthly maps revealed that its retrievals depict seasonal trends and patterns in concurrence with OMI and SBUV/2 observations (Divakarla et al., 2008). The validation of the AIRS TCO version 5 data for May-Sep. 2010 using high-precision ground-based TCO measurements by Brewer spectrophotometers, operated at world O_3 observation network stations Kislovodsk (43.7°N, 42.7°E) and Obninsk (55.1°N, 36.6°E) revealed the value of correlation coefficient (r) was 0.85 (the 95% confidence interval is 0.80–0.89) for Obninsk and 0.91 (0.88–0.93) for Kislovodsk station (Sitnov and Mokhov, 2016).

https://doi.org/10.5194/amt-2020-194
Preprint. Discussion started: 2 July 2020

2.2 MLS SCO and O_3 profile retrievals

The MLS instrument on-board Aura satellite, which was launched on 15 July 2004 and placed into a near-polar Earth orbit at 705 km with an inclination of 98°, uses the microwave limb sounding technique to measure vertical profiles of chemical constituents and dynamical tracers between the upper troposphere and the lower mesosphere (Waters et al., 2006). Its orbital ascending mode is at 13:42 (local solar time) and the orbital descending mode at 01:42 (local solar time) over 60°S-60°N. In this study, we use the MLS v4.2x standard O_3 product (2005-2018). Its retrieval is using 240-GHz radiance, providing near-global spatial coverage (82°S to 82°N latitude), with each profile spaced 1.5 degrees or ~165 km along the orbit track. This O_3 product includes the O_3 profile on 55 pressure surfaces and the recommended useful vertical range is from 261 to 0.02 hPa. In addition, it contains an O_3 column, which is the integrated stratospheric column down to the thermal tropopause calculated from MLS measured temperature (Livesey et al., 2015). Jiang et al. (2007) found the MLS stratospheric O_3 data between 120 and 3 hPa agreed well with ozonesonde measurements, within 8% for the global daily average. Froidevaux et al. (2008) reported MLS stratospheric O_3 uncertainties of the order of 5%, with values closer to 10% (and occasionally 20%) at the lowest stratospheric altitudes, where small positive biases are found. Livesey et al. (2008) found MLS O_3 accuracy was estimated at ~40 ppbv or +5% (~20 ppbv or +20% at 215 hPa). Comparisons with expectations and other observations show good agreements for the MLS O_3 product, generally consistent with the systematic errors quoted above.

3 Results

3.1 AIRS TCO day-night differences

Figure 1 shows spatial variations in the differences between the AIRS day and night measurements. Generally, 90% of the world's AIRS TCO is smaller during nighttime compared to daytime, and the decline over land is larger than over oceans indicating differences in surface loss. Seasonal averaged O_3 day-to-night relative difference shown in Figures 1a to 1d reveal that AIRS TCO day and night difference variations in Asia, Europe and North America during winter in the Northern Hemisphere (DJF) are smaller than during summer-time (JJA), in line with the efficient of photochemical production between seasons in the Northern Hemisphere. The Sahara Desert shows maximum difference value during winter-time when there are large day-night temperature differences. The same phenomenon is observed in Western Australia at summer-time.

In Figure 1e shows for the annual mean large differences of AIRS TCO retrievals over deserts, the Intertropical Convergence Zone (ITCZ) with persistent clouds and Arctic regions. These are regions with atypical earth surface properties or oceanic regions with persistent cloud cover. The spatial patterns over land mimic regions with low IR surface emissivity and/or regions where IR surface emissivity exhibits large seasonal variations (Feltz et al., 2018). Figure 1f shows significant TCO changes at the land-ocean interface. All these effects are important parameters for the retrieval algorithm but bear no physical relation with total O_3. Hence, the differences shown in Figure 1 provide strong indications that the largest AIRS day-

https://doi.org/10.5194/amt-2020-194
Preprint. Discussion started: 2 July 2020

Atmospheric Measurement Techniques Discussions

night TCO differences are dominated by retrieval artefacts. As such changes are unphysical, it confirms the hypothesis that clouds and the surface type (land/desert/vegetation/snow or ice) affects the AIRS TCO retrievals.

The AIRS emissivity retrieval uses the NOAA regression emissivity product as a first guess over land. The NOAA approach is based on clear radiances simulated from the European Centre for Medium-Range Weather Forecasts (ECMWF) forecast and a surface emissivity training data set (Goldberg et al., 2003). The training data set used for the AIRS V4 algorithm has a limited number of soil, ice, and snow types and very little emissivity variability in the training ensemble. In the AIRS V5 version, the regression coefficient set has been upgraded using a number of published emissivity spectra (12 spectra for ice/snow, 14 for land) blended randomly for land and ice (Zhou et al., 2008). These improvements generated a better emissivity first guess for use with the AIRS V5, and improved retrievals over the desert regions (Divakarla et al., 2008). In AIRS V6, a surface climatology was constructed from the 2008 monthly MODIS MYD11C3 emissivity product, and extended to the AIRS IR frequency hinge points using the baseline-fit approach described by Seemann et al. (2008). Nevertheless, using of day-night differences for evaluation of the AIRS V6 O_3 product suggest that further refinements for better surface emissivity retrievals are required and cloud covers is another problem that needs to be solved.

3.2 MLS O_3 retrievals day-night differences

3.2.1 MLS O_3 profile day-night differences

In order to better understand day-night differences in TCO, we also study day-night changes in the vertical profile of O_3 using MLS O_3 profile measurements. Figure 2a shows that the global (60 °S-60 °N) differences between day and night MLS O_3 profile occur in the mesosphere (10 hPa - 0.1 hPa). The O_3 mixing ratios are about an order of magnitude larger during night in the mesosphere, which was revealed by Huang et al. (2008) previously. Different latitude bands (30 degree) between 60 °S and 60 °N all display similar results.

We also find an unexpected polar bias at high latitudes in Figure 2d and 2g. On the one hand, the larger differences between ascending and descending MLS O_3 profile at high latitude extend from the stratosphere to the mesosphere. On the other hand, ascending O_3 is smaller than that at descending at 10 hPa over 60 °N-90 °N in Figure 2d, which is in contrast with the result of other latitude bands.

3.2.2 MLS O_3 retrievals in 90 °S-60 °S and 60 °N-90 °N

The MLS O_3 profile polar bias mentioned above turns out to be related to an inconsistency in the 'AscDescMode' flag of MLS v4.2x standard O_3 product in 90 °S-60 °S and 60 °N-90 °N. When this flag has a value of plus one or minus, it means an ascending or descending observation mode. We counted the daily number of pixels at both poles for which the flag has a value of plus one or minus one. Figures 3a and 3c show there is a clear change on 14 may 2015 in the daily number of ascending/descending pixels, consistent with the change of MLS SCO in Figure 3b and 3d. Before 14 may 2015, there are very large differences (about 500 pixels) in the number of pixels between ascending and descending mode, as well as the differences

https://doi.org/10.5194/amt-2020-194
Preprint. Discussion started: 2 July 2020

Atmospheric Measurement Techniques Discussions

in MLS SCO. After 14 may 2015, the ascending and descending MLS SCO are much closer with smaller differences (about 20 pixels) of ascending and descending pixels.

For the MLS O_3 profile in Figure 4, differences between ascending and descending MLS O_3 profiles at high latitudes for 2016-2018 are much smaller and more realistic compared to the differences for 2005-2014. The large differences in the stratosphere disappear in polar regions with the correct 'AscDescMode' flag for 2016-2018. For 60 °N-90 °N, ascending mode O_3 also becomes larger than descending mode O_3 at 10 hPa in Figure 4b. This indicates that the MLS 'AscDescMode' flag is correct for 2016-2018.

The O_3 retrieval algorithm adopted by the MLS v2.2 products has been validated to be highly accurate using multiple correlative measurements and the data have been used widely (Jiang et al., 2007; Froidevaux et al., 2008). The MLS v3.3 and v3.4, O_3 profile was reported on a finer vertical grid and the bottom pressure level with scientifically reliable values increases from 215 to 261 hPa (Livesey et al., 2015). The latest MLS v4.2x O_3 profile used in this study, released in February 2015, were in general similar to the previous version. One of the major improvements of MLS v4.2x was the handling of contamination from cloud signals in trace gas retrievals that resulted in significant reduction in the number of spurious MLS profile in cloudy regions and a more efficient screening of cloud-contaminated measurements. Furthermore, the MLS O_3 products have been improved through additional retrieval phases and reduction in interferences from other species (Livesey et al., 2015). We find no indications that changes in instrument or algorithm are responsible for this 'AscDescMode' flag inconsistency. This flag inconsistency is not present between 60 °S and 60 °N.

3.3 Comparison of AIRS TCO with MLS SCO and MLS O_3 profiles

Figure 5 presents yearly and monthly averaged TCO and SCO for 2005-2018 observed by AIRS and MLS three latitude bands. Figure 5a shows the 14-years averaged daytime AIRS TCO and MLS SCO in 60 °S-60 °N for 2005-2018. The time average MLS SCO column is 260.62 DU and AIRS TCO is 288.54 DU. It should be noted the MLS SCO is calculated from the stratosphere down to the thermal tropopause, while AIRS measures the TCO down to the surface. This explains why MLS SCO is almost 28 DU smaller than the AIRS TCO. The average MLS SCO day-night differences for 2005-2018 (0.88 DU) is smaller than the AIRS TCO day-night differences observed for the same time period (4.89 DU). The day-night difference of MLS SCO is 0.79 DU in the mesosphere (10 hPa - 0.1 hPa) and 0.03 DU in the stratosphere (100 hPa - 10 hPa). Compared to the AIRS TCO day-night differences, the magnitude of MLS SCO day-night differences in the stratosphere and in the mesosphere are much smaller. Figures 5c to 5f also confirm that MLS SCO has a polar bias when compared with AIRS TCO at high latitude.

3.4 Day-night difference of equatorial Pacific low O_3 regions

Generally, the Pacific low O_3 region (TCO < 220 DU) exist all year round and its size is larger at night than during the day, unlike the seasonal O_3 hole which occurs over Antarctica during the Southern Hemisphere polar winter. On the one hand, there are limited direct NOx emissions that is why O_3 low over oceans compared to land. On the other hand, the low O_3 over

https://doi.org/10.5194/amt-2020-194
Preprint. Discussion started: 2 July 2020

the tropical western Pacific can be attributed to tropospheric O_3 loss in this area. Its presence is related to a pronounced minimum in the tropospheric column of O_3 over the west Pacific, which exists due to efficient loss of photochemical mechanism with higher air temperatures and higher water concentrations for O_3. In addition, high sea surface temperatures also favour strong convective activity in the tropical West Pacific, which can lead to low O_3 mixing ratios in the convective outflow regions in the upper troposphere in spite of the increased lifetime of odd oxygen (Kley et al., 1996; Rex et al., 2014). A further reduction in the tropospheric O_3 burden through bromine and iodine emitted from open-ocean marine sources has been postulated by numerical models (Vogt et al., 1999; von Glasow et al., 2002; von Glasow et al., 2004; Yang et al., 2005) and observations (Read et al., 2008).

Figure 6a and 6c show the low O_3 region is mainly located over the western Pacific by AIRS. Rajab et al. (2013) investigated similar low TCO in Malaysia using AIRS data. They found the highest O_3 concentration occurred in April and May and the lowest O_3 concentration occurred during November and December, which is consistent with our result in Figure 6f. They also found that O_3 concentrations exhibited an inverse relationship with rainfall, but was positively correlated with temperature. MLS results show that the daytime low O_3 region also exists mainly in tropical western Pacific.

However, we find the occurrence frequency and intensity of low O_3 regions is higher at night by AIRS TCO and MLS SCO retrievals. Especially for MLS, the low O_3 regions appear in large areas at night besides in tropical western Pacific. For AIRS, clouds over oceans may have greater impact on the AIRS TCO retrievals at night. For MLS, more active chemical reactions may occur in these low O_3 regions at night.

For past, current and future monitoring of atmospheric phenomena like the Pacific tropospheric low O_3 area, it is important that observations are sufficient accurate. The evaluation of day-night differences in both MLS and AIRS has revealed the existence of biases in the satellite data that are sufficiently large in comparison to expected variations and changes in atmospheric O_3 that they may hamper the use of these satellite data studying them.

4 Conclusions

Comparison of daytime and nighttime AIRS TCO has revealed small but not insignificant biases in AIRS TCO. The differences are likely related to surface type (land/desert/vegetation/snow or ice) and infrared surface emissivity, especially over regions that exhibit smaller infrared emissivity or large seasonal variability in infrared emissivity. Differences typically were of the order of a few percent, which is significant given that long term changes in TCOs related to anthropogenic emissions of stratospheric O_3 depleting substances outside of polar regions are also of the order of a few percent.

There were major changes to the surface emissivity retrieval in AIRS V6 compared to previous versions resulting in a very significant improvement in yield and accuracy for surface temperature and emissivity over land and ice surfaces compared to previous versions. Nevertheless, our results indicate that the AIRS V6 TCO still can be further improved. In addition, AIRS TCO differences over oceans bear a clear cloud cover signature which is likely related to uncertainties in the representation of

https://doi.org/10.5194/amt-2020-194
Preprint. Discussion started: 2 July 2020

clouds in the retrieval algorithm. The latter may also impact AIRS TCO retrievals over land, although detection of cloud features in AIRS TCO day-night differences is difficult due to the presence of the land surface emissivity related bias.

The MLS v4.2x was very useful for verification of daytime and nighttime SCO and O_3 profile between 60 °S-60 °N. MLS day-night differences in SCO and O_3 profiles show that day-night differences are only small (< 1 DU for the upper atmospheric SCO), expect in the upper stratosphere and mesosphere. However, an inconsistency was found in the 'AscDescMode' flag in 60 °N-90 °N and in 90 °S-60 °S, resulting in inconsistent profiles in these regions before 14 May 2015. In processor version v4.22 and later versions this issue has been fixed, but since it is a relatively small issue, the MLS data set before 2016 has not been reprocessed.

Comparison of AIRS TCO and MLS SCO in 60 °S-60 °N for 2005-2018 showed the values of MLS SCO were lower than AIRS TCO because the MLS SCO was based on the stratosphere only. MLS SCO day-night difference in the stratosphere (0.03 DU) and in the mesosphere (0.79 DU) was much smaller compared with AIRS TCO day-night difference (4.89 DU). As shown in Smith et al. (2015) the lifetime of O_3 due to chemistry is strongly altitude dependent. Only in the mesosphere the timescale becomes low enough to see significant differences between average daytime and nighttime concentrations. Figures S1 to S4 indicate that AIRS TCO retrieval artefacts dominate the day/night variability of tropospheric O_3 residuals (TOR = AIRS TCO – MLS SCO) and the relatively small day-night differences of tropospheric O3 are hard to discriminate comparing day/night TCO.

We found that the frequency and intensity of low O_3 regions between 60 °S and 60 °N was higher at night by AIRS and MLS. The daytime low O_3 in tropical western Pacific was investigated, including its extent and causes. In order to clarify whether the more serious low O_3 regions at night are due to the problem of the algorithm itself or the atmospheric physical and chemical factors different from that in the daytime, we compared both MLS and AIRS at day and at night. It is necessary to verify day-night differences by infrared TCO observations for retrieval aspect first. Our results show that maintaining the quality of the satellite observations of stratospheric O_3 is therefore highly relevant.

Data availability

Satellite data sets used in this research can be requested from public sources. AIRS total ozone column data are available online (https://giovanni.gsfc.nasa.gov/giovanni/). The MLS Level 2 data can be obtained from the NASA Goddard Space Flight Center Data and Information Services Center (GSFCDISC, https://disc.gsfc.nasa.gov/datasets/ML2O3_004/summary?keywords=ML2O3_004).

Author contributions

WNW and JL provided satellite data, tools, and analysis. RA, JL and THC undertook the conceptualization and investigation. WNW prepared original draft. RA and JL carried out review and editing. JW checked the English language. All authors discussed the results and commented on the paper.

Competing interests

The authors declare that they have no conflict of interest.

Acknowledgements

The support provided by China Scholarship Council (CSC) during a visit of Wannan Wang to Royal Netherlands Meteorological Institute (KNMI) is acknowledged.

References

American Meteorological Society: https://www.ametsoc.org/index.cfm/ams/publications/bulletin-of-the-american-meteorological-society-bams/state-of-the-climate/, access: April 13 2020.

Ball, W. T., Alsing, J., Mortlock, D. J., Staehelin, J., Haigh, J. D., Peter, T., Tummon, F., Stubi, R., Stenke, A., Anderson, J., Bourassa, A., Davis, S. M., Degenstein, D., Frith, S., Froidevaux, L., Roth, C., Sofieva, V., Wang, R., Wild, J., Yu, P. F., Ziemke, J. R., and Rozanov, E. V.: Evidence for a continuous decline in lower stratospheric ozone offsetting ozone layer recovery, Atmos Chem Phys, 18, 1379-1394, 2018.

Ball, W. T., Alsing, J., Staehelin, J., Davis, S. M., Froidevaux, L., and Peter, T.: Stratospheric ozone trends for 1985–2018: sensitivity to recent large variability, Atmos. Chem. Phys., 19, 12731-12748, 10.5194/acp-19-12731-2019, 2019.

Barnett, J., Houghton, J., and Pyle, J.: The temperature dependence of the ozone concentration near the stratopause, Q J Roy Meteor Soc, 101, 245-257, 1975.

Brown, S. S., Neuman, J. A., Ryerson, T. B., Trainer, M., Dube, W. P., Holloway, J. S., Warneke, C., de Gouw, J. A., Donnelly, S. G., Atlas, E., Matthew, B., Middlebrook, A. M., Peltier, R., Weber, R. J., Stohl, A., Meagher, J. F., Fehsenfeld, F. C., and Ravishankara, A. R.: Nocturnal odd-oxygen budget and its implications for ozone loss in the lower troposphere, Geophys Res Lett, 33, 2006.

Brühl, C., Drayson, S. R., Russell, J. M., Crutzen, P. J., McInerney, J. M., Purcell, P. N., Claude, H., Gernandt, H., McGee, T. J., and McDermid, I. S.: Halogen Occultation Experiment ozone channel validation, Journal of Geophysical Research: Atmospheres, 101, 10217-10240, 1996.

Chapman, S.: A theory of upperatmospheric ozone, Mem. Roy. Meteor., 3, 103-125, 1930.

Chipperfield, M. P., Bekki, S., Dhomse, S., Harris, N. R. P., Hassler, B., Hossaini, R., Steinbrecht, W., Thieblemont, R., and Weber, M.: Detecting recovery of the stratospheric ozone layer, Nature, 549, 211-218, 2017.

Connor, B. J., Siskind, D. E., Tsou, J., Parrish, A., and Remsberg, E. E.: Ground-based microwave observations of ozone in the upper stratosphere and mesosphere, Journal of Geophysical Research: Atmospheres, 99, 16757-16770, 1994.

Craig, R. A., and Ohring, G.: The temperature dependence of ozone radiational heating rates in the vicinity of the mesopeak, Journal of Meteorology, 15, 59-62, 1958.

Cunnold, D., Chu, W., Barnes, R., McCormick, M., and Veiga, R.: Validation of SAGE II ozone measurements, Journal of Geophysical Research: Atmospheres, 94, 8447-8460, 1989.

Divakarla, M., Barnet, C., Goldberg, M., Maddy, E., Irion, F., Newchurch, M., Liu, X. P., Wolf, W., Flynn, L., Labow, G., Xiong, X. Z., Wei, J., and Zhou, L. H.: Evaluation of Atmospheric Infrared Sounder ozone profiles and total ozone retrievals with matched ozonesonde measurements, ECMWF ozone data, and Ozone Monitoring Instrument retrievals, J Geophys Res-Atmos, 113, 2008.

Evans, W., and Llewellyn, E.: Measurements of mesospheric ozone from observations of the 1.27 µm band, Radio Science, 7, 45-50, 1972.

Feltz, M., Borbas, E., Knuteson, R., Hulley, G., and Hook, S.: The Combined ASTER and MODIS Emissivity over Land (CAMEL) Global Broadband Infrared Emissivity Product, Remote Sens Environ, 10, 1027, 2018.

Fioletov, V. E., Bodeker, G. E., Miller, A. J., McPeters, R. D., and Stolarski, R.: Global and zonal total ozone variations estimated from ground-based and satellite measurements: 1964-2000, J Geophys Res-Atmos, 107, 2002.

Frith, S. M., Bhartia, P. K., Oman, L. D., Kramarova, N. A., McPeters, R. D., and Labow, G. J.: Model-based climatology of diurnal variability in stratospheric ozone as a data analysis tool, Atmos. Meas. Tech., 13, 2733-2749, 10.5194/amt-13-2733-2020, 2020.

Froidevaux, L., Jiang, Y., Lambert, A., Livesey, N., Read, W., Waters, J., Browell, E., Hair, J., Avery, M., and McGee, T.: Validation of aura microwave limb sounder stratospheric ozone measurements, Journal of Geophysical Research: Atmospheres, 113, 2008.

Fu, D., Kulawik, S. S., Miyazaki, K., Bowman, K. W., Worden, J. R., Eldering, A., Livesey, N. J., Teixeira, J., Irion, F. W., Herman, R. L., Osterman, G. B., Liu, X., Levelt, P. F., Thompson, A. M., and Luo, M.: Retrievals of tropospheric ozone profiles from the synergism of AIRS and OMI: methodology and validation, Atmos Meas Tech, 11, 5587-5605, 2018.

Fussen, D., Vanhellemont, F., Bingen, C., and Chabrillat, S.: Ozone profiles from 30 to 110 km Measured by the Occultation Radiometer Instrument during the period Aug. 1992–Apr. 1993, Geophys Res Lett, 27, 3449-3452, 2000.

Goldberg, M. D., Qu, Y., McMillin, L. M., Wolf, W., Zhou, L., and Divakarla, M.: AIRS near-real-time products and algorithms in support of operational numerical weather prediction, IEEE Transactions on Geoscience Remote Sensing of Environment, 41, 379-389, 2003.

Gunson, M., Farmer, C. B., Norton, R., Zander, R., Rinsland, C. P., Shaw, J., and Gao, B. C.: Measurements of CH4, N2O, CO, H2O, and O3 in the middle atmosphere by the Atmospheric Trace Molecule Spectroscopy Experiment on Spacelab 3, Journal of Geophysical Research: Atmospheres, 95, 13867-13882, 1990.

Hays, P., and Roble, R. G.: Observation of mesospheric ozone at low latitudes, Planetary Space Science, 21, 273-279, 1973.

Huang, F. T., Reber, C. A., and Austin, J.: Ozone diurnal variations observed by UARS and their model simulation, Journal of Geophysical Research: Atmospheres, 102, 12971-12985, 1997.

Huang, F. T., Mayr, H. G., Russell, J. M., Mlynczak, M. G., and Reber, C. A.: Ozone diurnal variations and mean profiles in the mesosphere, lower thermosphere, and stratosphere, based on measurements from SABER on TIMED, J Geophys Res-Space, 113, 2008.

Jiang, Y., Froidevaux, L., Lambert, A., Livesey, N., Read, W., Waters, J., Bojkov, B., Leblanc, T., McDermid, I., and Godin-Beekmann, S.: Validation of Aura Microwave Limb Sounder Ozone by ozonesonde and lidar measurements, Journal of Geophysical Research: Atmospheres, 112, 2007.

Kaufmann, M., Gusev, O. A., Grossmann, K. U., Martin-Torres, F. J., Marsh, D. R., and Kutepov, A. A.: Satellite observations of daytime and nighttime ozone in the mesosphere and lower thermosphere, J Geophys Res-Atmos, 108, 2003.

Kley, D., Crutzen, P. J., Smit, H. G. J., Vomel, H., Oltmans, S. J., Grassl, H., and Ramanathan, V.: Observations of near-zero ozone concentrations over the convective Pacific: Effects on air chemistry, Science, 274, 230-233, 1996.

Livesey, N., Read, W., Wagner, P., Froidevaux, L., Lambert, A., Manney, G., Pumphrey, H., Santee, M., Schwartz, M., and Wang, S. J. A., JPL publication, USA: Earth Observing System (EOS) Aura Microwave Limb Sounder (MLS) version 4.2 x level 2 data quality and description document, JPL D-33509 rev. A, Jet Propulsion Laboratory, California Institute of Technology, Pasadena, California, 91109-8099, 2015.

Livesey, N. J., Filipiak, M. J., Froidevaux, L., Read, W. G., Lambert, A., Santee, M. L., Jiang, J. H., Pumphrey, H. C., Waters, J. W., Cofield, R. E., Cuddy, D. T., Daffer, W. H., Drouin, B. J., Fuller, R. A., Jarnot, R. F., Jiang, Y. B., Knosp, B. W., Li, Q. B., Perun, V. S., Schwartz, M. J., Snyder, W. V., Stek, P. C., Thurstans, R. P., Wagner, P. A., Avery, M., Browell, E. V., Cammas, J.-P., Christensen, L. E., Diskin, G. S., Gao, R.-S., Jost, H.-J., Loewenstein, M., Lopez, J. D., Nedelec, P., Osterman, G. B., Sachse, G. W., and Webster, C. R.: Validation of Aura Microwave Limb Sounder O3 and CO observations in the upper troposphere and lower stratosphere, J. Geophys. Res, 113, 10.1029/2007jd008805, 2008.

London , J.: Radiative energy sources and sinks in the stratosphere and mesosphere, Atmospheric Ozone and its Variation and Human Influences, 703, 1980.

Marsh, D. R., Skinner, W. R., Marshall, A. R., Hays, P. B., Ortland, D. A., and Yee, J. H.: High Resolution Doppler Imager observations of ozone in the mesosphere and lower thermosphere, Journal of Geophysical Research: Atmospheres, 107, ACH 7-1-ACH 7-12, 2002.

Mlynczak, M. G., and Drayson, S. R.: Calculation of infrared limb emission by ozone in the terrestrial middle atmosphere: 1. Source functions, Journal of Geophysical Research: Atmospheres, 95, 16497-16511, 1990.

Pallister, R. C., and Tuck, A. F.: The diurnal variation of ozone in the upper stratosphere as a test of photochemical theory, Q J Roy Meteor Soc, 109, 271-284, 10.1002/qj.49710946002, 1983.

Parrish, A., Boyd, I. S., Nedoluha, G. E., Bhartia, P. K., Frith, S. M., Kramarova, N. A., Connor, B. J., Bodeker, G. E., Froidevaux, L., Shiotani, M., and Sakazaki, T.: Diurnal variations of stratospheric ozone measured by ground-based microwave remote sensing at the Mauna Loa NDACC site: measurement validation and GEOSCCM model comparison, Atmos. Chem. Phys., 14, 7255-7272, 10.5194/acp-14-7255-2014, 2014.

Pittman, J. V., Pan, L. L., Wei, J. C., Irion, F. W., Liu, X., Maddy, E. S., Barnet, C. D., Chance, K., and Gao, R. S.: Evaluation of AIRS, IASI, and OMI ozone profile retrievals in the extratropical tropopause region using in situ aircraft measurements, J Geophys Res-Atmos, 114, 2009.

Prather, M. J.: Ozone in the upper stratosphere and mesosphere, Journal of Geophysical Research: Oceans, 86, 5325-5338, 10.1029/JC086iC06p05325, 1981.

Rajab, J. M., Lim, H., and MatJafri, M.: Monthly distribution of diurnal total column ozone based on the 2011 satellite data in Peninsular Malaysia, The Egyptian Journal of Remote Sensing Space Science, 16, 103-109, 2013.

Read, K. A., Mahajan, A. S., Carpenter, L. J., Evans, M. J., Faria, B. V. E., Heard, D. E., Hopkins, J. R., Lee, J. D., Moller, S. J., Lewis, A. C., Mendes, L., McQuaid, J. B., Oetjen, H., Saiz-Lopez, A., Pilling, M. J., and Plane, J. M. C.: Extensive halogen-mediated ozone destruction over the tropical Atlantic Ocean, Nature, 453, 1232-1235, 2008.

Rex, M., Wohltmann, I., Ridder, T., Lehmann, R., Rosenlof, K., Wennberg, P., Weisenstein, D., Notholt, J., Kruger, K., Mohr, V., and Tegtmeier, S.: A tropical West Pacific OH minimum and implications for stratospheric composition, Atmos. Chem. Phys., 14, 4827-4841, 2014.

Sakazaki, T., Fujiwara, M., Mitsuda, C., Imai, K., Manago, N., Naito, Y., Nakamura, T., Akiyoshi, H., Kinnison, D., Sano, T., Suzuki, M., and Shiotani, M.: Diurnal ozone variations in the stratosphere revealed in observations from the Superconducting Submillimeter-Wave Limb-Emission Sounder (SMILES) on board the International Space Station (ISS), J Geophys Res-Atmos, 118, 2991-3006, 2013.

Schanz, A., Hocke, K., and Kämpfer, N.: Daily ozone cycle in the stratosphere: global, regional and seasonal behaviour modelled with the Whole Atmosphere Community Climate Model, Atmos. Chem. Phys., 14, 7645-7663, 10.5194/acp-14-7645-2014, 2014.

Seemann, S. W., Borbas, E. E., Knuteson, R. O., Stephenson, G. R., and Huang, H.-L.: Development of a global infrared land surface emissivity database for application to clear sky sounding retrievals from multispectral satellite radiance measurements, Journal of Applied Meteorology Climatology, 47, 108-123, 2008.

Simpson, D., Arneth, A., Mills, G., Solberg, S., and Uddling, J.: Ozone - the persistent menace: interactions with the N cycle and climate change, Curr Opin Env Sust, 9-10, 9-19, 2014.

Sitnov, S. A., and Mokhov, I. I.: Satellite-derived peculiarities of total ozone field under atmospheric blocking conditions over the European part of Russia in summer 2010, Russian Meteorology and Hydrology, 41, 28-36, 2016.

Smith, A. K., and Marsh, D. R.: Processes that account for the ozone maximum at the mesopause, J Geophys Res-Atmos, 110, 2005.

Velders, G. J., Andersen, S. O., Daniel, J. S., Fahey, D. W., and McFarland, M.: The importance of the Montreal Protocol in protecting climate, Proceedings of the National Academy of Sciences, 104, 4814-4819, 2007.

Vogt, R., Sander, R., Von Glasow, R., and Crutzen, P. J.: Iodine chemistry and its role in halogen activation and ozone loss in the marine boundary layer: A model study, J Atmos Chem, 32, 375-395, 1999.

von Glasow, R., Sander, R., Bott, A., and Crutzen, P. J.: Modeling halogen chemistry in the marine boundary layer - 1. Cloud-free MBL, J Geophys Res-Atmos, 107, 2002.

von Glasow, R., von Kuhlmann, R., Lawrence, M. G., Platt, U., and Crutzen, P. J.: Impact of reactive bromine chemistry in the troposphere, Atmos. Chem. Phys., 4, 2481-2497, 2004.

Waters, J. W., Froidevaux, L., Harwood, R. S., Jarnot, R. F., Pickett, H. M., Read, W. G., Siegel, P. H., Cofield, R. E., Filipiak, M. J., and Flower, D. A.: The earth observing system microwave limb sounder (EOS MLS) on the Aura satellite, IEEE Transactions on Geoscience Remote Sensing, 44, 1075-1092, 2006.

Weeks, L., Good, R., Randhawa, J., and Trinks, H.: Ozone measurements in the stratosphere, mesosphere, and lower thermosphere during Aladdin 74, Journal of Geophysical Research: Space Physics, 83, 978-982, 1978.

WMO: Scientific Assessment of Ozone Depletion: 2010, Global Ozone Research and Monitoring Project-Report No. 52, Geneva, Switzerland, 516, 2011.

WMO: Scientific Assessment of Ozone Depletion: 2014, World Meteorological Organization, Global Ozone Research and Monitoring Project-Report No. 55, Geneva, Switzerland, 416, 2014.

WMO: Scientific Assessment of Ozone Depletion: 2018, Global Ozone Research and Monitoring Project – Report No. 58, Geneva, Switzerland, 588, 2018.

Yang, X., Cox, R. A., Warwick, N. J., Pyle, J. A., Carver, G. D., O'Connor, F. M., and Savage, N. H.: Tropospheric bromine chemistry and its impacts on ozone: A model study, J Geophys Res-Atmos, 110, 2005.

Zhou, L., Goldberg, M., Barnet, C., Cheng, Z., Sun, F., Wolf, W., King, T., Liu, X., Sun, H., and Divakarla, M.: Regression of surface spectral emissivity from hyperspectral instruments, IEEE Transactions on Geoscience Remote Sensing of Environment, 46, 328-333, 2008.

Zommerfelds, W., Kunzi, K., Summers, M., Bevilacqua, R., Strobel, D., Allen, M., and Sawchuck, W.: Diurnal variations of mesospheric ozone obtained by ground-based microwave radiometry, Journal of Geophysical Research: Atmospheres, 94, 12819-12832, 1989.

https://doi.org/10.5194/amt-2020-194
Preprint. Discussion started: 2 July 2020

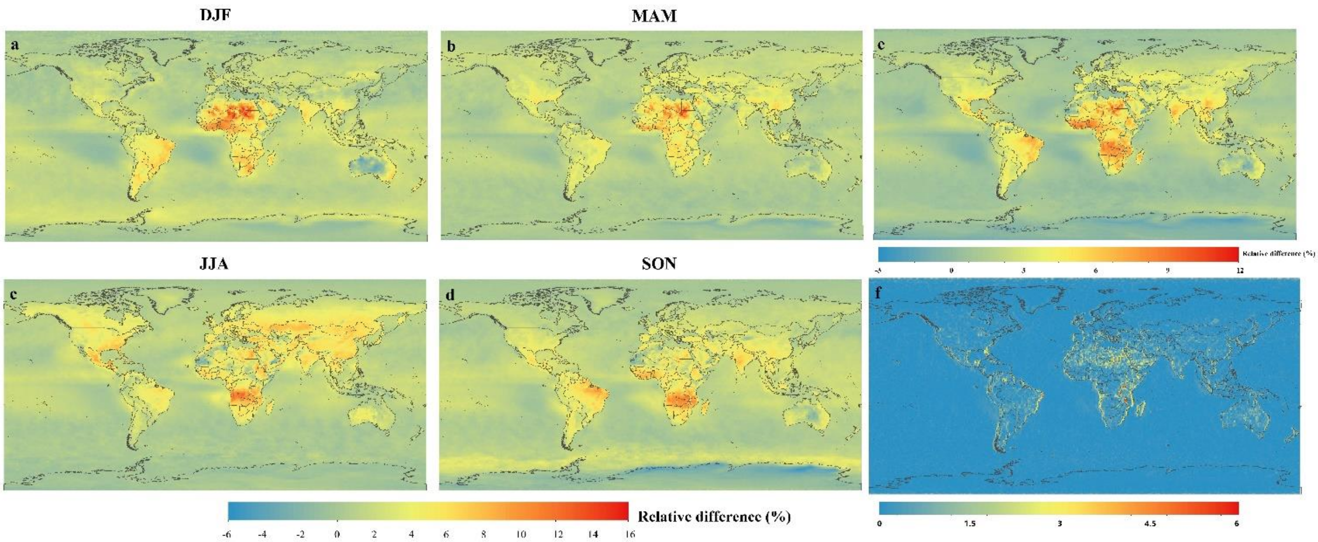

Figure 1: AIRS TCO averaged day-to-night relative difference for 2003-2018. The relative difference is calculated as: 100 × (daytime - nighttime) / daytime (in percent, %). (a) DJF. (b) MAM. (c) JJA. (d) SON. (e) 16 years averaged. (f) longitude gradient value using absolute difference between two pixels adjacent at the same latitude in (e).

https://doi.org/10.5194/amt-2020-194
Preprint. Discussion started: 2 July 2020

Atmospheric Measurement Techniques
Discussions

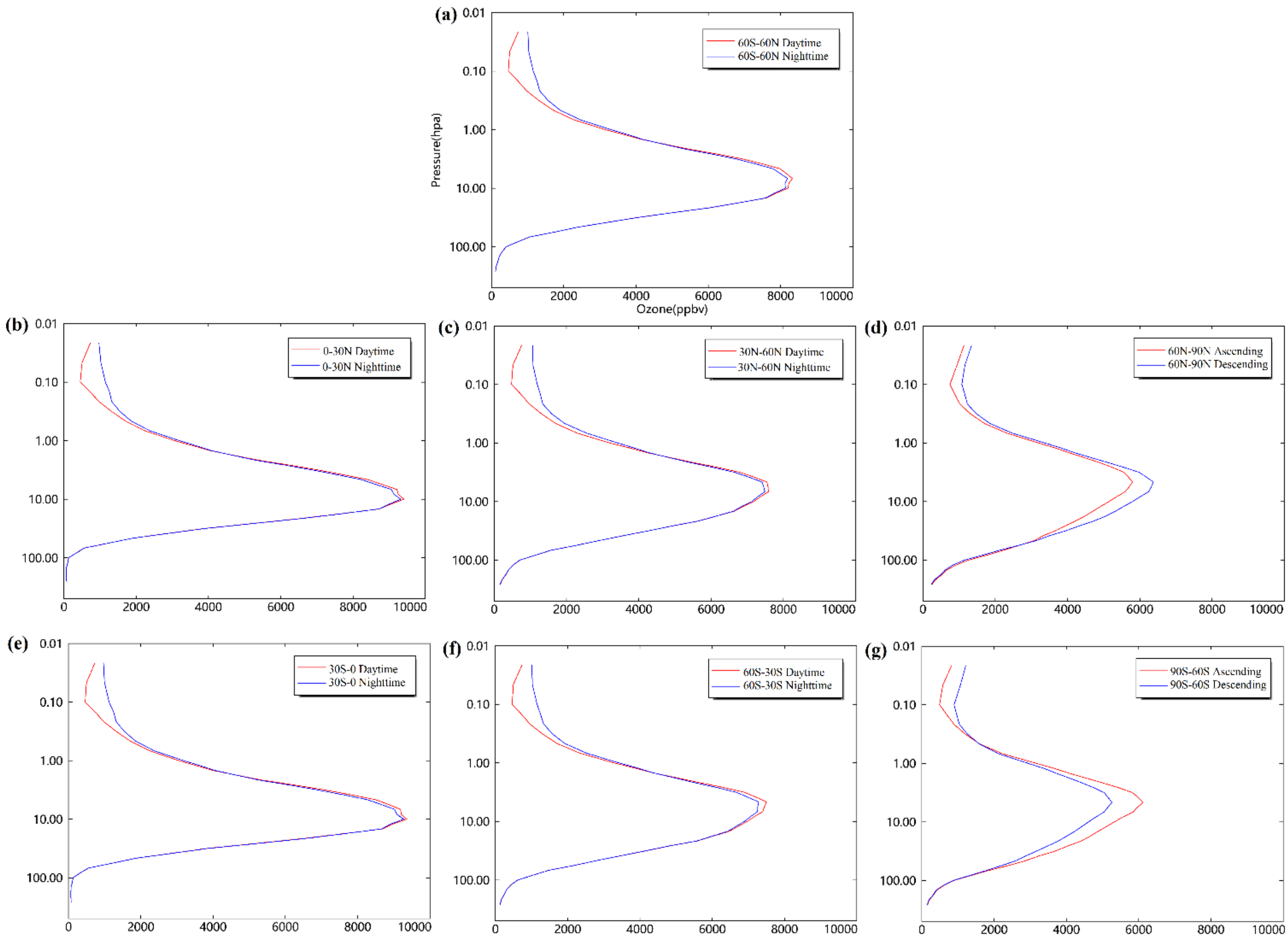

Figure 2: Averaged MLS ozone profile between 261 hPa and 0.02 hPa per latitude band (30 degree) for 2005-2018. (a) 60 °S-60 °N. (b) 0-30 °N. (c) 30 °N-60 °N. (d) 60 °N-90 °N. (e) 30 °S-0. (f) 60 °S-30 °S. (g) 90 °S-60 °S.

https://doi.org/10.5194/amt-2020-194
Preprint. Discussion started: 2 July 2020

Atmospheric Measurement Techniques
Discussions

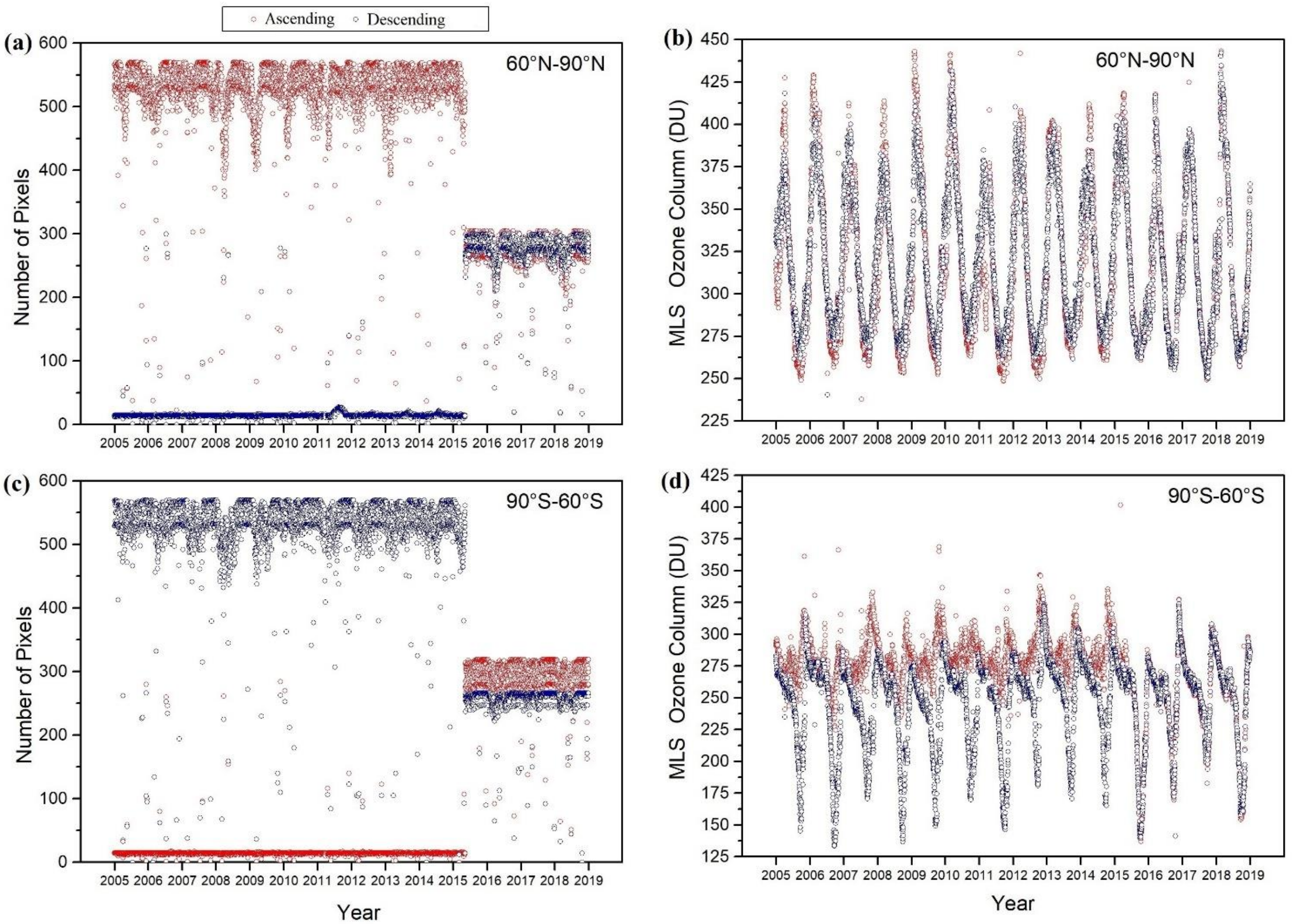

Figure 3: (a) Time series of daily number of Ascending and Descending pixels in 60 °N-90 °N. (b) Time series of daily average Ascending and Descending MLS SCO in 60 °N-90 °N. (c) Same as (a), but in 90 °S-60 °S. (d) Same as (b), but in 90 °S-60 °S.

https://doi.org/10.5194/amt-2020-194
Preprint. Discussion started: 2 July 2020

Atmospheric Measurement Techniques Discussions

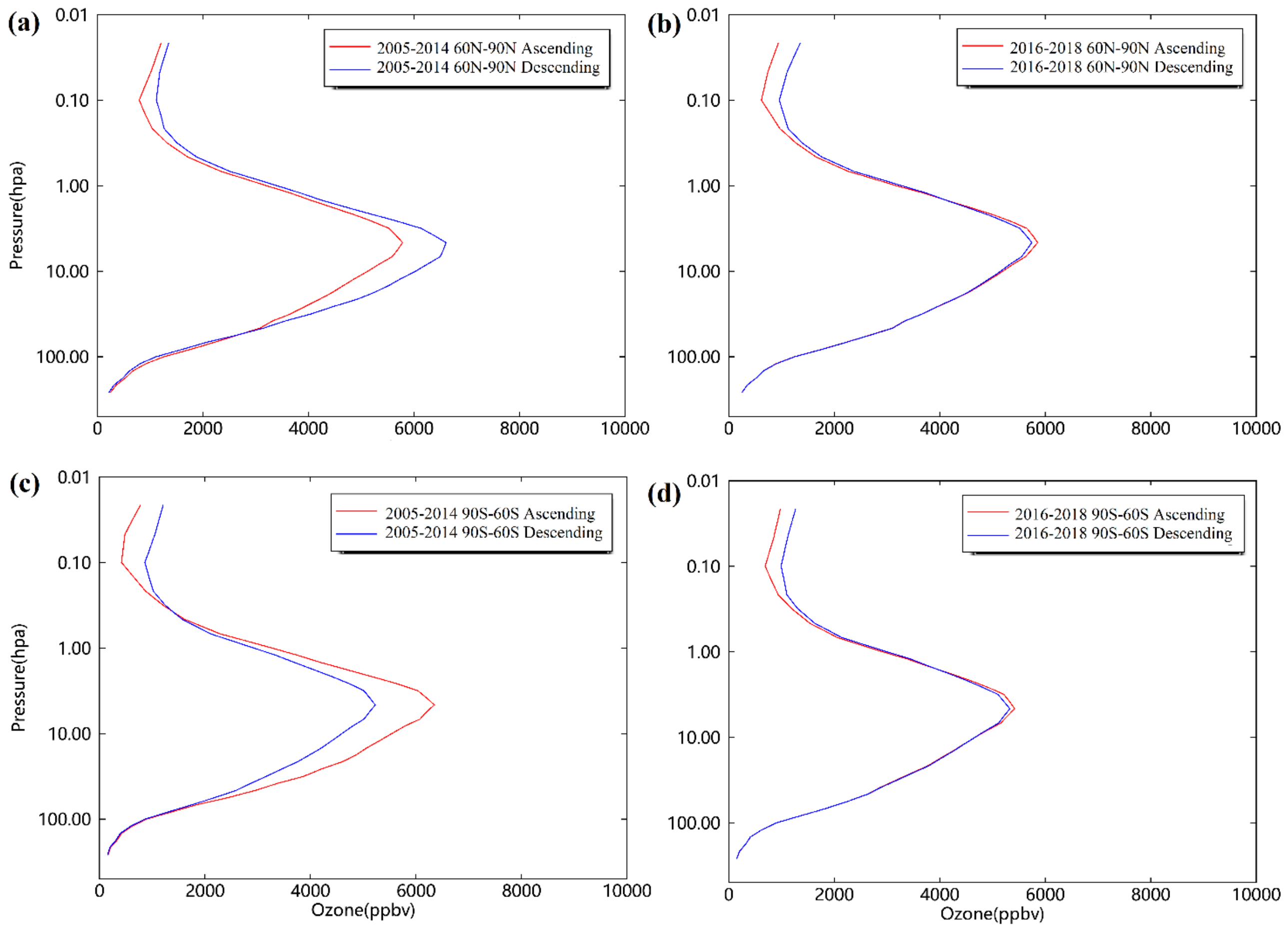

445 **Figure 4: (a) Averaged MLS ozone profile between 261 hPa and 0.02 hPa for 2005-2014 in 60 °N-90 °N. (b) Averaged MLS ozone profile between 261 hPa and 0.02 hPa for 2016-2018 in 60 °N-90 °N. (c) Same as (a), but in 90 °S-60 °S. (d) Same as (b), but in 90 °S-60 °S.**

https://doi.org/10.5194/amt-2020-194
Preprint. Discussion started: 2 July 2020

Atmospheric Measurement Techniques
Discussions

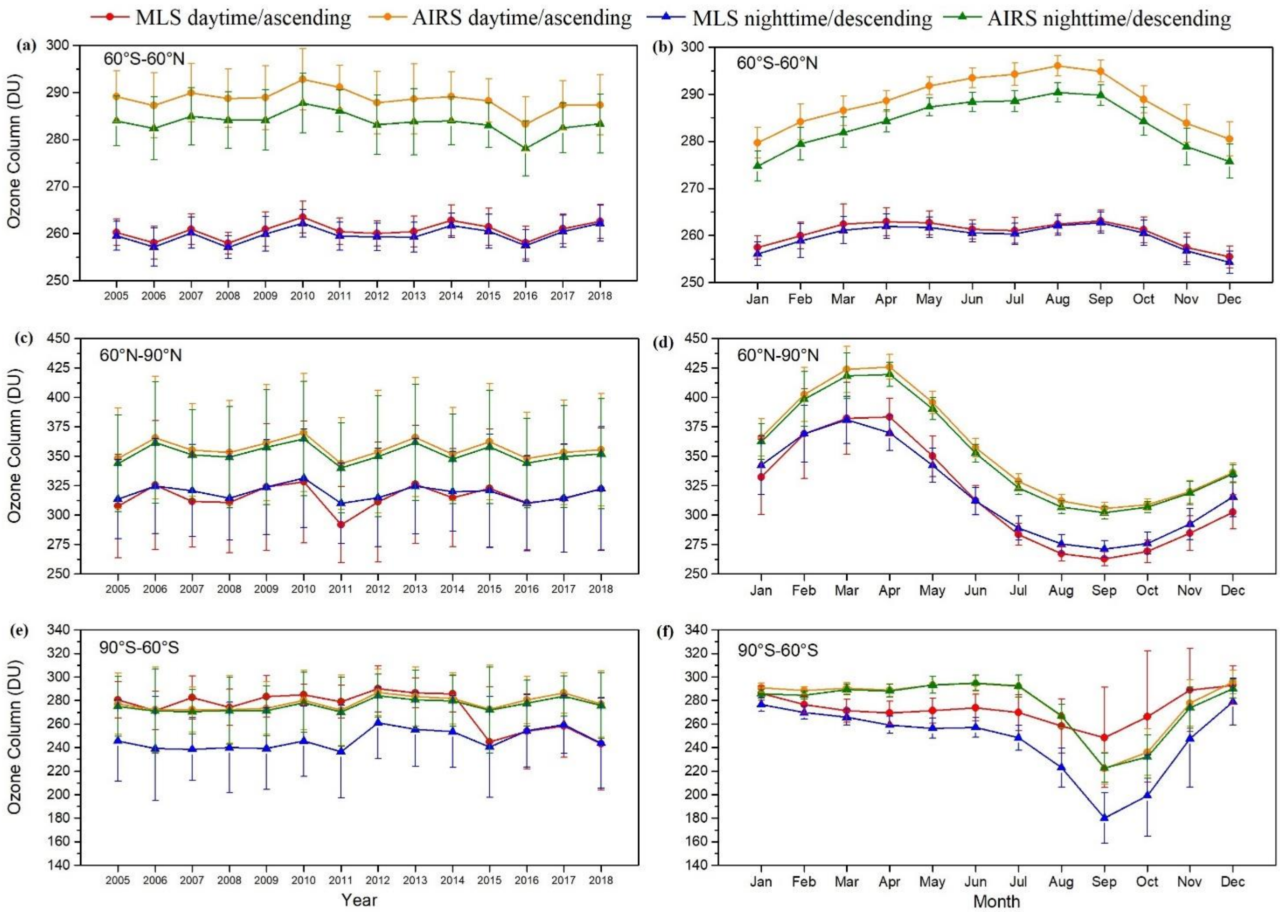

Figure 5: Yearly and monthly averaged AIRS TCO and MLS SCO for 2005-2018.

https://doi.org/10.5194/amt-2020-194
Preprint. Discussion started: 2 July 2020

Atmospheric Measurement Techniques Discussions

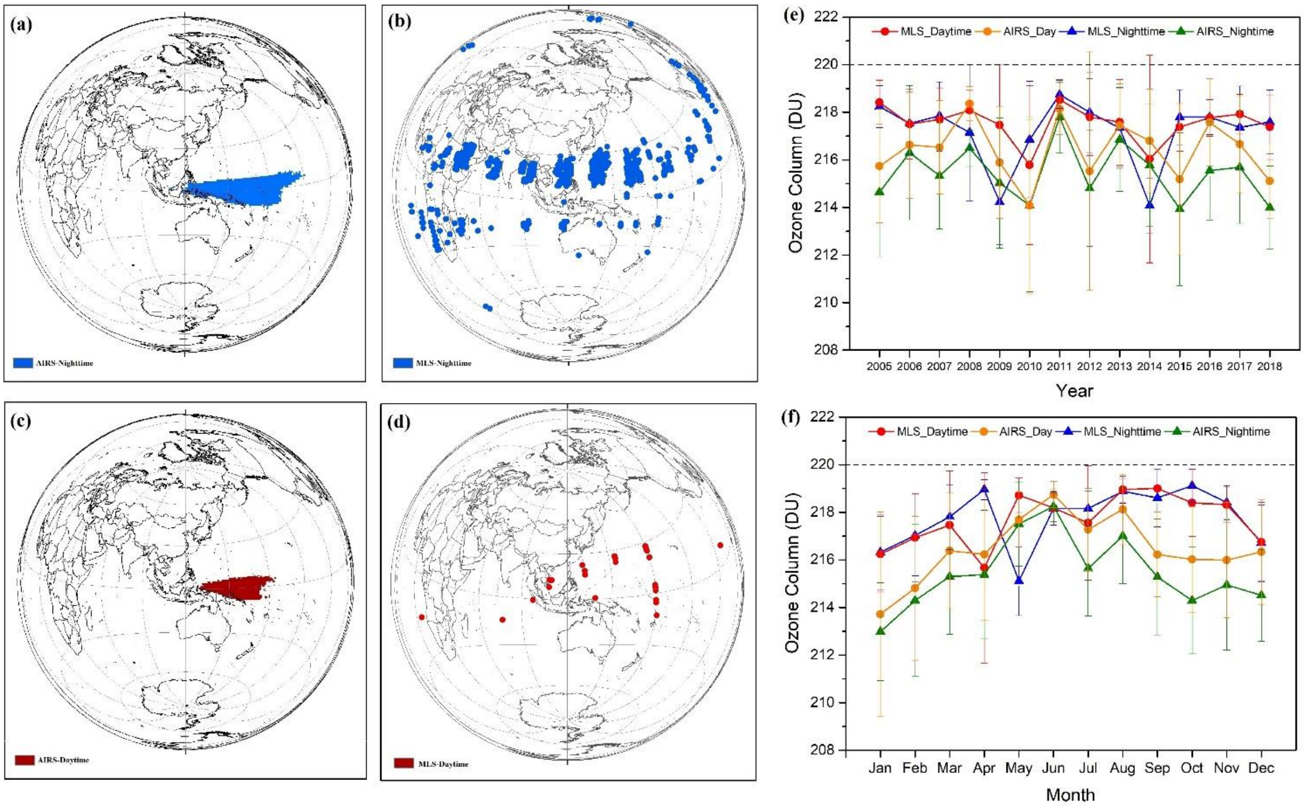

Figure 6: Spatial and temporal distribution of the low ozone. (a) Location (composite pixel) of the yearly nighttime low ozone from 2005 to 2018 for AIRS TCO. (b) Same as a but for MLS SCO. (c) Location (composite pixel) of the yearly daytime low ozone from 2005 to 2018 for AIRS TCO. (d) Same as c but for MLS SCO. (e) Yearly averaged AIRS TCO and MLS SCO of the low ozone regions for 2005-2018. (f) Monthly averaged AIRS TCO and MLS SCO of the low ozone regions for 2005-2018. Uncertainties represent the standard deviation of the measured values.